This manuscript was published by Superconductor Science & Technology (SuST, IOP) 27, No. 4, 044009, (2014).

Critical current anisotropy in Nd-1111 single crystals and the influence of neutron irradiation

M. Eisterer, V. Mishev, and M. Zehetmayer

Atominstitut, Vienna University of Technology,

Stadionallee 2, 1020 Vienna, Austria

N. D. Zhigadlo

Laboratory for Solid State Physics, ETH Zurich, CH-8093 Zurich, Switzerland

S. Katrych and J. Karpinski

Laboratory for Solid State Physics, ETH Zurich, CH-8093 Zurich, Switzerland and

Institute of Condensed Matter Physics,

EPFL, CH-1015 Lausanne, Switzerland

Abstract

We report on angle-resolved magnetization measurements on Nd-1111 single crystals. The field dependence of the critical current density, J_c, is non-monotonous in these crystals at all orientations and temperatures due to the fishtail effect, which strongly influences the angular dependence of J_c. The currents decrease as the field is tilted from the crystallographic c-axis at low fields, but increase at high fields. A peak occurs in the angular dependence of J_c at intermediate fields. The critical currents are significantly enhanced after irradiation with fast neutrons and the fishtail disappears. The different current anisotropies at low and high fields, however, persist. We discuss the data in the framework of the anisotropic scaling approach and propose a transition from dominant pinning by large defects of low density at low fields to pinning by small defects of high density at high fields in the pristine crystal. Strong pinning dominates at all fields after the irradiation, and the angular dependence of J_c can be described by anisotropic scaling only after an appropriate extension to this pinning regime.

This manuscript was published by Superconductor Science & Technology (SuST, IOP) 27, No. 4, 044009, (2014).

I. INTRODUCTION

The pinning properties of iron-based superconductors have been in the focus of intensive research since the discovery of superconductivity in these compounds.[1] Many similarities to the cuprates were found. The critical currents in single crystals often show a fishtail effect, which disappears after the introduction of an efficient pinning landscape, for instance by irradiation techniques.[2–7] In thin films on the other hand, pinning is much stronger and the currents decrease monotonously with field.[8–23] Angle-resolved measurements of the pinning properties are very efficient for studying the pinning landscape and anisotropy effects of the vortex lattice. They were performed nearly exclusively on films so far, in which growth-related and often correlated defects dominate the properties, which are not representative for the defects prevailing in bulk materials such as single crystals or grains in wires or tapes. Angle-resoved measurements on crystals are thus highly desirable to complement the film data. Thin films are widely available only of the Ba-122 ($BaFe_2As_2$) [8–15] and 11 ($FeSe_{1-x}Te_x$) [16–20] families and only a few data exist for the 1111 (LaFeAsO) family.[21–23] The latter has the highest anisotropy among them, [24] which makes it the best candidate for studying anisotropy effects. Anisotropy is considered as a key parameter for applications, since it enhances the harmful thermal fluctuations. In this study we report on the anisotropy of the in-plane critical currents of Nd-1111 single crystals by angle-resolved magnetization measurements. The results are discussed in the framework of the anisotropic scaling approach.[25] After the characterization of the pristine crystals the defect structure was changed completely by irradiation with fast neutrons to assess changes in the pinning properties arising from the introduced pinning centers.

II. EXPERIMENTAL

The Nd-1111 single crystals were prepared by a high pressure technique.[26] Two crystals were studied, whose geometries were determined in two steps. First, an optical microscope was used to establish the lateral surface area. A subsequent mass measurement enabled the calculation of the volume and the thickness of the samples from the theoretical mass density.[27] The results are listed in Table I. The transition temperature (T_c) was measured in a 1 T SQUID by applying an AC field of 0.3 mT. The reported transition temperature

This manuscript was published by Superconductor Science & Technology (SuST, IOP) 27, No. 4, 044009, (2014).

refers to the onset of superconductivity, where the susceptibility starts to deviate from its behavior in the normal conducting state.

Sample	a (mm)	b (mm)	c (mm)
Nd1111#1	0.633	0.401	0.058
Nd1111#2	0.497	0.36	0.0309

TABLE I. Sample geometries

Magnetization loops were recorded on crystal #1 at different temperatures in a 7 T SQUID with the field applied parallel to the *c*-axis of the sample. The critical current density, J_c, along the *ab*-planes was evaluated from the irreversible magnetic moment m_{irr}. A self-field correction was applied for the calculation of the average magnetic field B within the crystal.[28]

Sample #1 and #2 were irradiated to a fast neutron fluence ($E > 0.1\,\mathrm{MeV}$) of $3.7{\cdot}10^{21}\,\mathrm{m}^{-2}$ and $1.8{\cdot}10^{21}\,\mathrm{m}^{-2}$, respectively. The fluence was determined from the radioactivity of a nickel foil which was placed in the same quartz tube as the sample during the irradiation. Fast neutron irradiation is known to result in a variety of defects, ranging from single displaced atoms to spherical defect cascades of about 5 nm in diameter.[3, 29–31]

Angle-resolved magnetization measurements were performed on crystal #2 in a 5 T vector Vibrating Sample Magnetometer (VSM). Previous studies described similar measurements on superconducting thin films,[16, 32, 33] where the currents flow parallel to the lateral surface at all orientations. The measurements on crystals can be interpreted in the same way as long as the currents remain parallel to the *ab*-planes (the large surface). This condition was verified from the orientation of the magnetic moment, which is available in a vector VSM. The currents inside the sample were found to remain parallel to the large surface (and to the *ab*-planes) up to an angle of at least 80°, which is a consequence of the large aspect ratio of the crystal. Only data within this angular range will be considered in the following in order to avoid problems with currents flowing in arbitrary directions and the resulting change in geometry of the current loops. However, not all currents flow under Maximum Lorentz Force (MLF), when the sample is inclined from one of its main orientations, and the currents flowing under Variable Lorentz Force (VLF) potentially change the angular dependence of J_c.[16] Whenever the VLF-currents may influence the behavior in a qualitative way, it will

This manuscript was published by Superconductor Science & Technology (SuST, IOP) 27, No. 4, 044009, (2014).

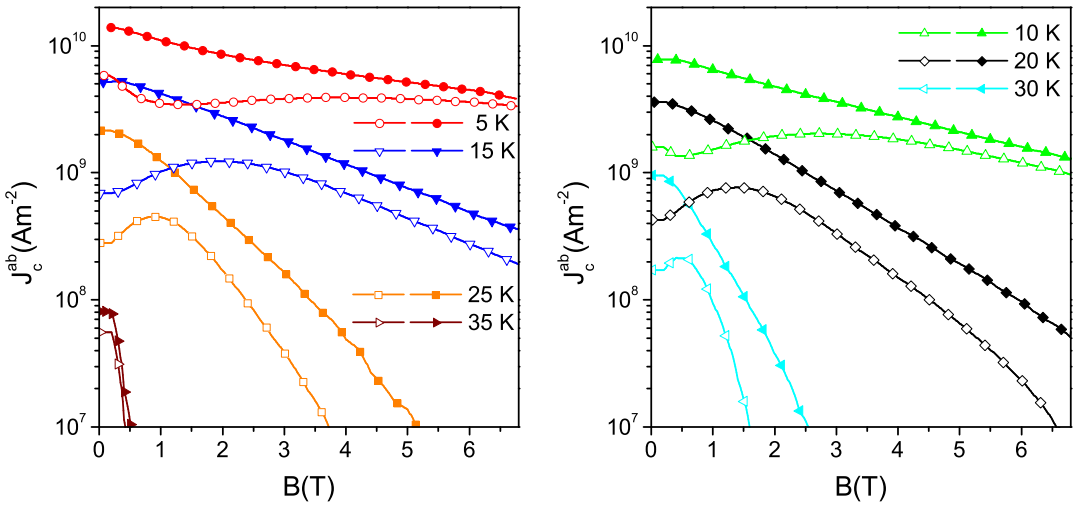

FIG. 1. Critical current densities of the Nd-1111 single crystal #1 at various temperatures as a function of the magnetic flux density ($B\|c$). The open and solid symbols refer to the pristine and the neutron irradiated crystal, respectively.

be noted explicitly. We will also restrict our considerations to 15 K where the VSM signal is sufficiently large ($> 10^{-7}$ Am^2), the self-field is comparatively small and the peak of the fishtail is visible in a wide angular range. At higher temperatures, the signal of the tiny crystals was too small for a careful analysis, at lower temperatures the self field increases and the fishtail moves out of the accessible field range (< 5 T) at rather low angles. However, the behavior did not change qualitatively at these temperatures.

III. RESULTS

The irradiation slightly reduces the transition temperature from 39.9 K to 39.3 K in crystal #1 ($3.7 \cdot 10^{21}\, m^{-2}$) and from 39.3 K to 39.1 K in crystal #2 ($1.8 \cdot 10^{21}\, m^{-2}$). These findings are consistent with previous reports on Sm-1111 bulk samples [3] or Ba-122 single crystals.[2] The modest decrease in T_c is also comparable with that in the cuprates [34, 35]. A small neutron fluence does not harm the transition temperature significantly, but improves pinning. (Note that superconductivity is totally suppressed after irradiation to a neutron fluence of the order of $10^{23}\, m^{-2}$.[36].)

Figure 1 shows the changes in critical current density upon neutron irradiation at var-

This manuscript was published by Superconductor Science & Technology (SuST, IOP) 27, No. 4, 044009, (2014).

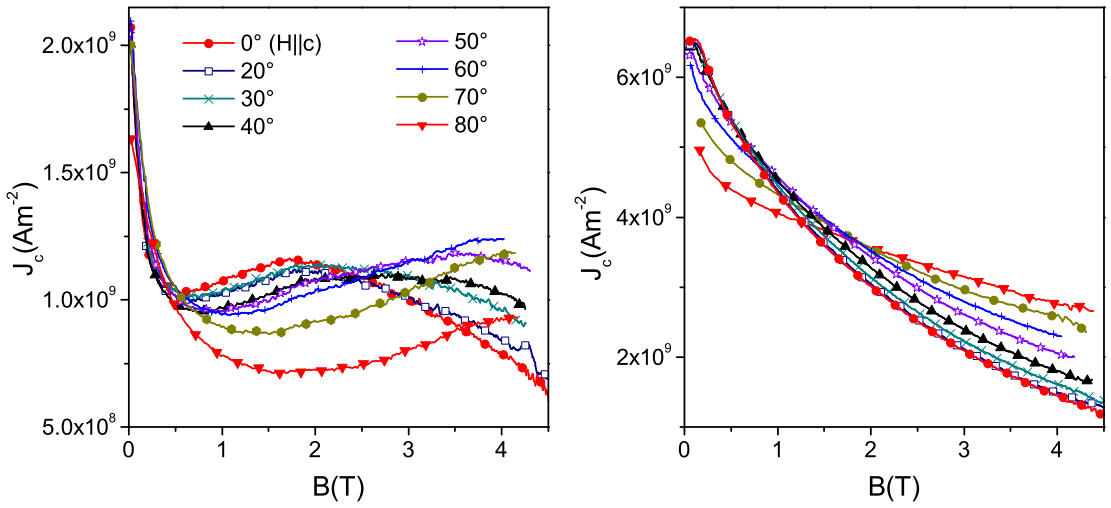

FIG. 2. Field dependence of the critical current density in crystal #2 at 15 K for various angles between the applied magnetic field and the crystallographic c-axis. Left panel: pristine crystal. Right panel: after irradiation to a fast neutron fluence of $1.8 \cdot 10^{21}\,\mathrm{m}^{-2}$

ious temperatures for the magnetic field applied parallel to the crystallographic c-axis. A strong increase in J_c, the disappearance of the fishtail (or second peak) effect and a shift of the irreversibility field at high temperatures are observed. This behavior resembles the corresponding changes in cuprate superconductors,[35, 37, 38] Sm-1111 bulk samples,[3] and Sm-1111 crystals irradiated with heavy ions.[39] In the latter case, the enhancement as well as the resulting currents are much higher, because this irradiation technique introduces larger defects and because of the higher transition temperature of those 1111 crystals, which were much closer to optimal doping than the crystals of our study. In Co-doped Ba-122 single crystals on the other hand, the irreversibilty fields tend to decrease at high temperatures after fast neutron irradiation, while similar J_c-enhancements were found.[2]

Next, we consider the anisotropy of the critical currents including the influence of disorder. The field dependence of J_c at 15 K and varying crystal orientation is shown in Fig. 2. α denotes the angle between the applied magnetic field and the crystallographic c-axis, thus $\alpha = 0$ refers to $H \| c$. In the left panel (pristine crystal), the position of the "fishtail"-peak shifts to higher magnetic fields at larger α and the peak value of J_c grows for $\alpha \gtrsim 50°$. Below the peak field, the currents decrease with α, in contrast to expectations for uncorrelated pinning centers in an anisotropic superconductor. At high fields, the "usual" behavior, i.e.

This manuscript was published by Superconductor Science & Technology (SuST, IOP) 27, No. 4, 044009, (2014).

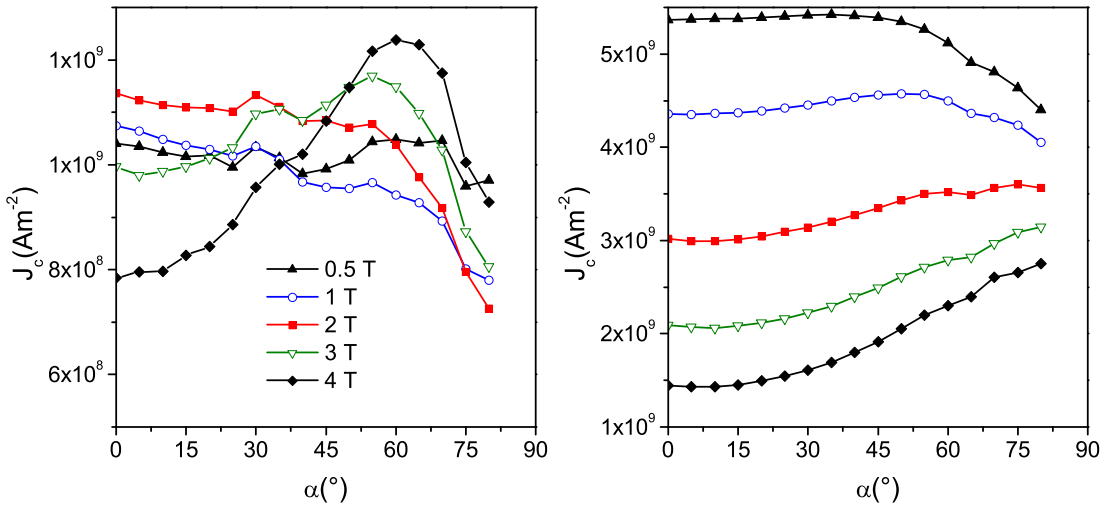

FIG. 3. Angular-dependence of the critical currents (crystal #2) at 15 K prior to (left) and after (right) irradiation.

growing currents with increasing α, is found. The angular dependence of J_c is plotted in Fig. 3 for a better illustration of the change in behaviour. A peak occurs in $J_c(\alpha)$ at 3 and 4 T, because these fields are above and below the position of the "fishtail"-peak at low ($\lesssim 40°$) and high angles ($\gtrsim 65°$), respectively.

Although J_c becomes monotonous with field after irradiation, a similar transition from the "unusual" behavior at low fields to the expected behavior at high fields is observed (right panel in Fig. 3), since the $J_c(B)$ curves cross each other (right panel in Fig. 2).

IV. DISCUSSION

The current standard approach for modelling anisotropy effects in superconductors was proposed by Blatter et al. more than two decades ago.[25] The main idea of this approach consists of scaling all relevant superconducting properties by functions of $\epsilon(\alpha)$, which is given by

$$\epsilon(\alpha) = \sqrt{\gamma^{-2}\sin^2(\alpha) + \cos^2(\alpha)} \tag{1}$$

The anisotropy parameter γ originally refers to the anisotropy of the effective mass of the charge carriers but is usually determined by the anisotropy of the upper critical field (i.e. $\gamma = B_{c2}^{ab}/B_{c2}^{c}$, where the indices ab and c refer to the crystallographic ab-planes and c-axis,

This manuscript was published by Superconductor Science & Technology (SuST, IOP) 27, No. 4, 044009, (2014).

respectively). In particular, the angular dependence of the upper critical field becomes $B_{c2}(\alpha) = B^c_{c2}/\epsilon(\alpha)$, as predicted by anisotropic Ginzburg-Landau theory, thus motivating the anisotropic scaling approach. This behavior is widely observed in many classes of superconductors, although multi-band [40, 41] or two-dimensional [42] superconductivity may cause deviations. Available data on the iron based superconductors [2, 43] suggest its validity also in this new family. The irreversibilty fields are expected to share the same angular dependence ($B_{irr}(\alpha) = B^c_{irr}/\epsilon(\alpha)$), if pinning is not too anisotropic. Since B_{irr} defines the field where J_c becomes zero, it is obvious that the angular dependence of J_c at high fields (close to B_{irr}) has to be dominated by the behavior of B_{irr} itself. This is indeed observed in both, the pristine and irradiated crystal.

The scaling law for J_c is less obvious because J_c is given by the (extrinsic) pinning properties. The original prediction of the anisotropic scaling approach is based on the collective pinning theory, which was proposed for a high density of weak pinning sites. In this case and if the currents flow parallel to the *ab*-planes, only the field has to be scaled: $J_c(B, \alpha) = J_c(B\epsilon(\alpha), 0)$. This means that the field virtually decreases if the sample is rotated from 0 to 90°. If the currents decrease with field (as usual), they increase with α. Due to the fishtail effect in the pristine samples of our study the currents *increase* with field in a certain field range, where the scaling approach results in *decreasing* currents at increasing α. However, this does not explain all features of the angular dependence observed in the unirradiated crystal, as discussed in the following.

The data of Fig. 2 are replotted as a function of the scaled field ($B\epsilon(\alpha)$) in Fig. 4 in order to sort out the effect of field scaling. If the scaling approach works properly, we expect that $J_c(B\epsilon)$ in the right panel has the same slope at all angles, which is indeed obtained for $\gamma = 3.5$. This value also seems realistic in view of the available data, i.e. γ is 5-8 near T_c and decreases with temperature.[21, 44, 45]

Although the field scaling brings the minima and maxima of J_c close together, the curves do not collapse (left panel in Fig. 4). The positions of the maxima do not coincide, which could be caused by a higher anisotropy in the unirradiated crystal. It also seems that the value of J_c at the second maximum increases at large angles, but this might be an artifact of the measurement method (VLF currents). On the other hand, the decrease of the J_c-minimum with α cannot be caused by VLF currents and agrees with the overall behavior of the angular dependence of J_c in the irradiated crystal.

This manuscript was published by Superconductor Science & Technology (SuST, IOP) 27, No. 4, 044009, (2014).

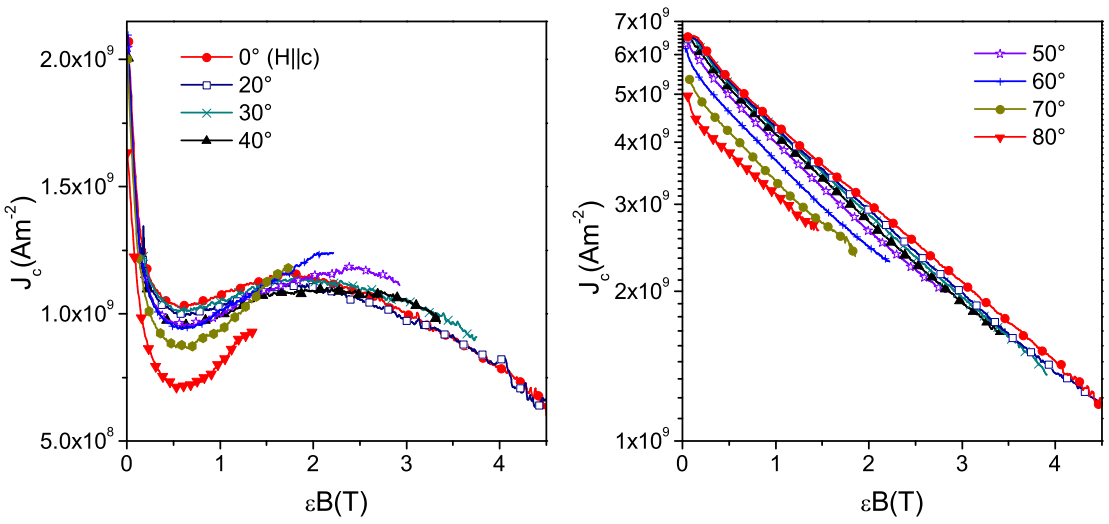

FIG. 4. Same data as in Fig. 2 but with field scaling assuming an anisotropy γ of 3.5.

Scaling of J_c in the irradiated crystals can be performed by $J_c(B,\alpha) = A_J(\epsilon(\alpha))J_c(B\epsilon(\alpha),0)$, with an a priori unknown function $A_J(\alpha)$ (or $A_J(\epsilon(\alpha))$). (Note that this scaling fails at very low fields, where the self field rotates B within the sample toward the c-axis. This is an artifact of our evaluation, because the applied self field correction only calculates the absolute value of B. Although correcting for α was possible, it would impede plotting $J_c(B,\alpha)$ without interpolation between measurements at different angles.) $A_J(\alpha)$ is expected to be constant [25] within the single vortex pinning regime of collective pinning theory, where the defects are assumed to be smaller than the coherence length ξ. In a simple model, the pinning energy of a single defect becomes proportional to $E_c r_d^3$, with the condensation energy density E_c and the defect radius r_d. Therefore, the pinning energy does not depend on α. If the defects are larger than the coherence length, the pinning energy becomes proportional to $E_p \propto E_c r_d \xi_{ab}\xi(\alpha) = E_c r_d \xi_{ab}^2/\epsilon(\alpha)$, thus decreases with α. This qualitatively explains our data on the irradiated crystal, although a direct scaling with pinning energy $A_J(\alpha) \propto E_p(\alpha)$ is not consistent with our data, when assuming a realistic systematic error caused by the VLF currents. However, a direct proportionality between pinning energy and critical current density is not expected from most pinning models, in particular in view of the changing elastic properties of the vortex lattice when the field orientation changes. Scaling by the square root of the pinning energy leads to reasonable agreement of all data, but a quantitative analysis of the angular dependence of A_J is not meaningful because of

This manuscript was published by Superconductor Science & Technology (SuST, IOP) 27, No. 4, 044009, (2014).

the systematic error of angular resolved magnetization measurements.

The angular dependence of A_J should not be related to a particular superconductor, but generally result from large pinning centers. Indeed, a decreasing J_c with increasing α was also observed in neutron irradiated coated conductors [46] before the intrinsic peak close to $H\|ab$ occurs and only if the field is significantly below B_{irr}.

The fishtail effect induces additional complexity into the angular dependence of J_c (e.g. left panel of Fig. 3, which can be understood by field scaling (see above).) However, we find a crossover in $A_J(\alpha)$, which decreases with α at low fields, but increases at higher fields, in particular near the second peak. The behavior near and above the second peak is essentially consistent with the predictions of the anisotropic scaling approach,[25] if one assumes the anisotropy to be a little higher and relates the slightly different currents at the peak to the peculiarities of the measurement method. At low fields on the other hand, the currents decrease with α, as in the irradiated crystal. The crossover suggests that pinning in the pristine crystals is dominated by comparatively large defects of low density at low fields and by small defects of high density at high magnetic fields.

V. CONCLUSIONS

The angular dependence of the critical currents was derived from magnetization measurements of Nd-1111 single crystals. The fishtail effect and the introduction of disorder change the current anisotropy significantly. It was demonstrated that the originally proposed pure field scaling resulting from collective pinning theory is valid only in a limited field range. However, the concept can be extended to other pinning regimes by introducing an additional J_c-scaling, which was motivated by the expected anisotropy of the pinning energy. This extension is mandatory for J_c at low fields in the unirradiated sample and in the whole field range after fast neutron irradiation, since pinning is dominated by large defects in these cases.

ACKNOWLEDGMENTS

We wish to thank H. W. Weber for fruitful discussions. This work was supported by the Austrian Science Fund (FWF): P22837-N20 and by the European-Japanese collaborative

This manuscript was published by Superconductor Science & Technology (SuST, IOP) 27, No. 4, 044009, (2014).

project SUPER-IRON (No. 283204).

---

[1] Kamihara Y., Watanabe T., Hirano M., and Hosono H. 2008 *J. Am. Chem. Soc.* **130** 3296

[2] Eisterer M., Zehetmayer M., Weber H. W., Jiang J., Weiss J. D., Yamamoto A., and Hellstrom E. E. 2009 *Supercond. Sci. Technol.* **22** 095011

[3] Eisterer M., Weber H. W., Jiang J., Weiss J. D., Yamamoto A., Polyanskii A. A., Hellstrom E. E., and Larbalestier D. C. 2009 *Supercond. Sci. Technol.* **22** 065015

[4] Prozorov R., Tanatar M. A., Roy B., Ni N., Bud'ko S. L., Canfield P. C., Hua J., Welp U., and Kwok W. K. 2010 *Phys. Rev.* B **81** 094509

[5] Fang L., Jia Y., Chaparro C., Sheet G., Claus H., Kirk M. A., Koshelev A. E., Welp U., Crabtree G. W., Kwok W. K., Zhu S., Hu H. F., Zuo J. M., Wen H.-H., and Shen B. 2012 *Appl. Phys. Lett.* **101** 012601

[6] Tamegai T., Taen T., Yagyuda H., Tsuchiya Y., Mohan S., Taniguchi T., Nakajima Y., Okayasu S., Sasase M., Kitamura H., Murakami T., Kambara T., and Kanai Y. 2012 *Supercond. Sci. and Technol.* **25** 084008

[7] Shahbazi M., Wang X. L., Ghorbani R. S., Ionescu M., Shcherbakova O. V., Wells F. S., Pan A. V., Dou S. X., and Choi K. Y. 2013 *Supercond. Sci. Technol.* **26** 095014

[8] Lee S., Jiang J., Zhang Y., Bark C. W., Weiss J. D., Tarantini C., Nelson C. T., Jang H. W., Folkman C. M., Baek S. H., Polyanskii A., Abraimov D., Yamamoto A., Park J. W., Pan X. Q., Hellstrom E. E., Larbalestier D. C., and Eom C. B. 2010 *Nat. Mater.* **9** 397

[9] Hänisch J., Iida K., Haindl S., Kurth F., Kauffmann A., Kidszun M., Thersleff T., Freudenberger J., Schultz L., and Holzapfel B. 2011 *IEEE Trans. Appl. Supercond.* **21** 2887

[10] Iida K., Hänisch J., Trommler S., Haindl S., Kurth F., Ruben Hühne R., Schultz L., and Holzapfel B. 2011 *Supercond. Sci. Technol.* **24** 125009

[11] Maiorov B., Katase T., Baily S. A., Hiramatsu H., Holesinger T. G., Hosono H., and Civale L. 2011 *Supercond. Sci. Technol.* **24** 055007

[12] Haberkorn N., Maiorov B., Usov I. O., Weigand M., Hirata W., Miyasaka S., Tajima S., Chikumoto N., Tanabe K., and Civale Leonardo 2012 *Phys. Rev. B* **85** 014522

[13] Maiorov B., Katase T., Usov I. O., Weigand M., Civale L., Hiramatsu H., and Hosono H. 2012 *Phys. Rev.* B **86** 094513

[14] Tarantini C., Lee S., Kametani F., Jiang J., Weiss J. D., Jaroszynski J., Folkman C. M., Hellstrom E. E., Eom C. B., and Larbalestier D. C. 2012 *Phys. Rev.* B **86** 214504

[15] Miura M., Maiorov B., Kato T., Shimode T., Wada K., Adachi S., and Tanabe K. 2013 *Nature Comm.* **4** 2499

[16] Eisterer M., Raunicher R., Weber H. W., Bellingeri E., Cimberle M. R., Pallecchi I., Putti M., and Ferdeghini C. 2011 *Supercond. Sci. Technol.* **24** 065016

[17] Bellingeri E., Kawale S., Braccini V., Buzio R., Gerbi A., Martinelli A., Putti M., Pallecchi I., Balestrino G., Tebano A., and Ferdeghini C. 2012 *Supercond. Sci. Technol.* **25** 084022

[18] Mele P., Matsumoto K., Fujita K., Yoshida Y., Kiss T., Ichinose A., and Mukaida M. 2012 *Supercond. Sci. and Technol.* **25** 084021

[19] Chen Li, Tsai C.-F., Zhu Y., Chen A., Bi Z., Lee J., and Wang H. 2012 *Supercond. Sci. Technol.* **25** 025020

[20] Iida K., Hänisch J., Reich E., Kurth F., Hühne R., Schultz L., Holzapfel B., Ichinose A., Hanawa M., Tsukada I., Schulze M., Aswartham S., Wurmehl S., and Büchner B. 2013 *Phys. Rev.* B **87** 104510

[21] Kidszun M., Haindl S., Thersleff T., Hänisch J., Kauffmann A., Iida K., Freudenberger J., Schultz L., and Holzapfel B. 2011 *Phys. Rev. Lett.* **106** 137001

[22] Takeda S., Ueda S., Takano S., Yamamoto A., and Naito N. 2012 *Supercond. Sci. Technol.* **25** 035007

[23] Iida K., Hänisch J., Tarantini C., Kurth F., Jaroszynski J., Ueda S., Naito M., Ichinose A., Tsukada I., Reich E., Grinenko V., Schultz L., and Holzapfel B. 2013 *Sci. Rep.* **3** 2139

[24] Putti M., Pallecchi I., Bellingeri E., Cimberle M. R., Tropeano M., Ferdeghini C., Palenzona A., Tarantini C., Yamamoto A., Jiang J., Jaroszynski J., Kametani F., Abraimov D., Polyanskii A., Weiss J. D., Hellstrom E. E., Gurevich A., Larbalestier D. C., Jin R., Sales B. C., Sefat A. S., McGuire M. A., Mandrus D., Cheng P., Jia Y., Wen H. H., Lee S., and Eom C. B. 2010 *Supercond. Sci. Technol.* **23** 034003

[25] Blatter G., Geshkenbein V. B., and Larkin A. I. 1992 *Phys. Rev. Lett.* **68** 875

[26] Zhigadlo N. D., Weyeneth S., Katrych S., Moll P. J. W., Rogacki K., Bosma S., Puzniak R., Karpinski J., and Batlogg B. 2012 *Phys. Rev.* B **86** 214509

[27] Karpinski J., Zhigadlo N. D., Katrych S., Bukowski Z., Moll P., Weyeneth H., Puzniak R., Tortello M., Daghero D., Gonnelli R., Maggio-Aprile I., Fasano Y., Fischer Ø., Rogacki K.,

This manuscript was published by Superconductor Science & Technology (SuST, IOP) 27, No. 4, 044009, (2014).

and Batlogg B. 2009 *Physica C* **469** 370

[28] Zehetmayer M. 2009 *Phys. Rev.* B **80** 104512

[29] Frischherz M. C., Kirk M. A., Zhang J. P., and Weber H. W. 1993 *Philos. Mag. A* **67** 1347

[30] Aleksa M., Pongratz P., Eibl O., Sauerzopf F. M., Weber T. W., and Kes P. H. 1998 *Physica C* **297** 171

[31] Chudy M., Eisterer M., W. Weber H., Veterníková J., Sojak S., and Slugeň V. 2012 *Supercond. Sci. Technol.* **25** 075017

[32] Thompson J. R., Sinclair J. W., Christen D. K., Zhang Y., Zuev Y. L., Cantoni C., Chen Y., and Selvamanickam V. 2010 *Supercond. Sci. Technol.* **23** 014002

[33] Hengstberger F., Eisterer M., and Weber H. W. 2011 *Supercond. Sci. Technol.* **24** 045002

[34] Sauerzopf F. M. 1998 *Phys. Rev.* B **57** 10959

[35] Weigand M., Eisterer M., Giannini E., and Weber H. W. 2010 *Phys. Rev.* B **81** 014516

[36] Karkin A. E., Werner J., Behr G., and Goshchitskii B. N. 2009 *Phys. Rev. B* **80** 174512

[37] Werner M., Sauerzopf F. M., Weber H. W., and Wisniewski A. 2000 *Phys. Rev. B* **61** 14795

[38] Wisniewski A., Puzniak R., Karpinski J., Hofer J., Szymczak R., Baran M., Sauerzopf F. M., Molinski R., Kopnin E. M., and Thompson J. R. 2000 *Phys. Rev.* B **61** 791

[39] Fang L., Jia Y., Mishra V., Chaparro C., Vlasko-Vlasov V. K., Koshelev U., Crabtree G. W., Zhu S., Katrych S., Zhigadlo N. D., Karpinski J., and Kwok W. K. 2013 *Nature Comm.* **4** 3655

[40] Gurevich A. 2003 *Phys. Rev.* B **67** 184515

[41] Arai M. and Kita T. 2005 *Physica C* **426-431** 179

[42] Marcon R., Silva E., Fastampa R., and Giura M. 1992 *Phys. Rev.* B **46** 3612

[43] Iida K., Hänisch J., Thersleff T., Kurth F., Kidszun M., Haindl S., Hühne R., Schultz L., and Holzapfel B. 2010 *Phys. Rev.* B **81** 100507

[44] Jaroszynski J. et al. 2008 *Phys. Rev.* B **78** 064511

[45] Jia Y., Cheng P., Fang L., Luo H., Yang H., Ren C., Shan L., Gu C. Gu, and Wen H.-Hu 2008 *Appl. Phys. Lett.* **93** 032503

[46] Eisterer M., Fuger R., Chudy M., Hengstberger F., and Weber H. W. 2010 *Supercond. Sci. Technol.* **23** 014009